Parallel Models for Arborescent Polyisobutylene Synthesized in Batch Reactor

Yutian R. Zhao and Kimberley B. McAuley
Dept. of Chemical Engineering, Queen's University, Kingston, ON, Canada K7L 3N6

Judit E. Puskas
Dept. of Chemical & Biomolecular Engineering, University of Akron, Akron, OH 44325

DOI 10.1002/aic.14655
Published online October 30, 2014 in Wiley Online Library (wileyonlinelibrary.com)

A mathematical model is developed for estimating kinetic parameters that influence the production of arborescent polyisobutylene via carbocationic copolymerization of inimer (IM) and isobutylene. Six different propagation rate constants arise due to the two types of vinyl groups and three types of carbocations. These six parameters are estimated using parallel simulation systems in PREDICI that track (1) functional groups, (2) internal and dangling segments in the polymer, and (3) concentrations of IM and polymer molecules. Parameter estimates obtained using the proposed model result in a better fit to literature data than was obtained using a previous model that neglected two types of propagations reactions. Predictions from the proposed model are consistent with Monte Carlo simulations for molecular weight distribution of the internal and dangling segments. © 2014 American Institute of Chemical Engineers *AIChE J*, 61: 253–265, 2015
Keywords: branching, carbocationic polymerization, parameter estimation, mathematical model, polyisobutylene

Introduction

Fréchet et al. invented self-condensing vinyl polymerization (SCVP) about two decades ago, greatly simplifying the synthesis process for arborescent or hyperbranched polymers.[1] In their SCVP system, an "inimer"(IM) is used to initiate the polymerization and induce branching. An IM molecule typically has two types of active sites: (1) an initiating site that can start propagation and (2) a vinyl group that can be polymerized to form a branching point. The IM used in this study is 4-(2-chloroiopropyl) styrene, shown in Figure 1a, which is produced *in situ* from 4-(2-methoxyisopropyl)styrene and $TiCl_4$.[3,4] Since the invention of SCVP, considerable research has been performed on related topics including: synthesizing polymers via self-condensing vinyl copolymerization (SCVCP),[3–10] developing different kinds of IM molecules and arborescent polymers[11–13] and building mathematical models for SCVP and SCVCP systems.[2,14–26] Puskas and coworkers.[27–29] developed a promising biomaterial via living block copolymerization of styrene on an *arborescent* polyisobutylene (*arb*PIB) core. This *arb*PIB core was synthesized through a "one-pot" living carbocationic copolymerization of isobutylene (IB) and IM molecules.[2] A simplified reaction scheme is shown in Figure 1b. This biomaterial can be used for human implantation (e.g., for breast implants) and has higher biocompatibility, better strength, and less permeability to liquids than silicone materials.[28,29]

In Puskas's "one-pot" living cationic polymerization, shown in Figure 1b, there are two types of vinyl groups V_I, V_M and three types of chloride end groups C_I, C_M, C_S as shown in Figure 1b. V_I is the vinyl group on IM, while V_M is the vinyl group on the IB monomer. A C_I end group is an unreacted chloride group on IM, a C_M end group forms after addition of a V_M group, and a C_S end group forms after the reaction of a V_I group. As a result, there are six different propagation rate constants, which are $k_{p\mathrm{II}}$, $k_{p\mathrm{IM}}$, $k_{p\mathrm{MI}}$, $k_{p\mathrm{MM}}$, $k_{p\mathrm{SI}}$, and $k_{p\mathrm{SM}}$, where the first subscript after k_p represents the type of end group that is uncapped for reaction, and the second subscript represents the type of vinyl group that is consumed. Table 1 summarizes all six reactions between different end groups and vinyl groups. The rate constants above the arrows in Table 1 are apparent rate constants that depend on equilibrium constants for capping and uncapping of chloride end groups and the corresponding true rate constants, as shown in Table 2. The expressions in Table 2 were developed using Puskas's two-path reaction scheme for carbocationic polymerization, which is shown in Figure 2 for a homopolymerization process.

In living carbocationic polymerization, there is a fast equilibrium between capped and uncapped chloride end groups, which occurs due to the presence of a Lewis acid (LA). Note that $TiCl_4$ is the LA used in the reaction mechanism shown in Figure 1b. According to Puskas and coworkers,[30–33] there are two paths for uncapping the chloride end groups. Path A is dominant when there is only a small amount of LA in the system, while path B is dominant when there is a large excess of LA in the system. Values of apparent rate constants $k_{p\mathrm{IMapp}}$, $k_{p\mathrm{MIapp}}$, $k_{p\mathrm{MMapp}}$, and $k_{p\mathrm{SMapp}}$ in Table 2 were estimated using our previous PREDICI model, which is only valid at

This contribution was identified by Dr. John R. Richards (E. I. du Pont de Nemours and Company) as the Best Presentation in the session "Modeling and Control of Polymer Processes: A Tribute to John P. Congalidis" of the 2013 AIChE Annual Meeting in San Francisco, CA.

Correspondence concerning this article should be addressed to K. B. McAuley at kim.mcauley@chee.queensu.ca.

© 2014 American Institute of Chemical Engineers

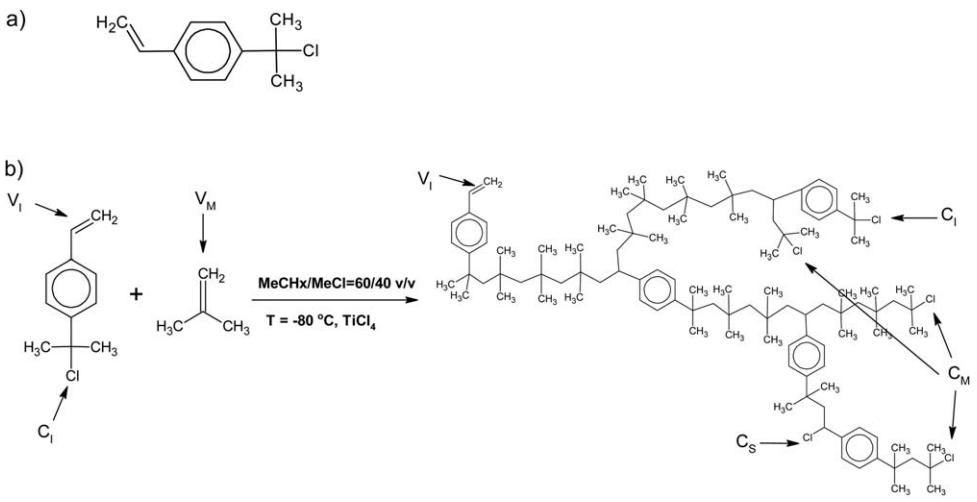

Figure 1. (a) Typical structure of an IM; (b) a simplified reaction mechanism of "one-pot" living copolymerization of IM and IB.[2]

very low branching levels using the experimental data of Dos Santos.[2,4] Values for $k_{p\mathrm{IIapp}}$ and $k_{p\mathrm{SIapp}}$, which were excluded from our previous model via simplifying assumptions, are reasonable nominal values that we used in Monte Carlo (MC) models to simulate detailed branching and molecular weight information.[14,15]

The average branching level in *arb*PIB can be calculated from[4]

$$B_{\mathrm{kin}} = \frac{\bar{M}_n}{\bar{M}_{n,\mathrm{theo}}} - 1 \tag{1}$$

$$\bar{M}_{n,\mathrm{theo}} = M_{\mathrm{IM}} + \frac{[\mathrm{IB}]_0 - [\mathrm{IB}]}{[\mathrm{IM}]_0 - [\mathrm{IM}]} M_{\mathrm{IB}} \tag{2}$$

where $\bar{M}_n$ is the number average molecular weight and $\bar{M}_{n,\mathrm{theo}}$ is the theoretical number average molecular weight, calculated for the situation where vinyl groups on IM are unable to react so that only linear IB chains are produced.

Puskas et al. showed that the physical properties of this *arb*PIB biomaterial are largely decided by its molecular weight distribution (MWD) and branching level.[6,34] Thus, building a model that can accurately predict these properties will be beneficial for designing future experiments to achieve targeted properties. Several research groups have built models for SCVP and SCVCP systems.[2,14–26] Many of these models rely on simplifying assumptions that may influence the accuracy of the model predictions.[16–26] SCVP and SCVCP models can be classified into two categories: (1) models that are based on dynamic material balance equations and (2) models that are based on MC simulations.

Müller et al. and Yan et al.[22–26] developed a series of models for SCVP and SCVCP systems using dynamic material balance equations. Their SCVP model[22,23] resulted in analytical expressions for MWD and branching level for IM homopolymerization in a batch reactor. To develop analytical expressions for average molecular weights and branching levels during SCVCP (i.e., copolymerization of IM and a vinyl monomer), they assumed that different types of propagation rate constants are equal. This assumption may not be valid for copolymerization of 4-(2-chloroisopropyl)styrene and IB, based on the chemical structures of the three carbocations involved.[2]

Cheng et al.[20,21] developed two SCVP models using dynamic material balances, which were solved using generating functions. Their first model assumed that the same value could be used for two different propagation rate constants (i.e., $k_{p\mathrm{IIapp}}$ and $k_{p\mathrm{SIapp}}$). In their second model, this assumption was relaxed.

Only a few research groups have performed MC simulations of SCVP or SCVCP systems. He et al.[17] built a MC model for a SCVP system using a multifunctional initiator in addition to the IM. In their SCVCP model,[19] equal reactivity assumptions were made for different types of end groups and different types of vinyl groups, which may lead to inaccurate predictions.

Our previous research on modeling of *arb*PIB used a combination of material balance models and MC models.[2,14,15] First, we built a dynamic material balance model using PREDICI, which tracks polymer chains according to the number of IM units and monomer units they contain, as well as the number of end-groups of different types.[2] Because of the prohibitive number of polymer species that needed to be tracked, several assumptions (shown in Table 3) were applied to keep the number of species and reactions manageable (i.e., 122 different species and 1430 reaction steps in PREDICI). This model should only be used for predicting MWD and branching levels when the average number of branches per molecule is small (i.e., <5) so that very few branched molecules contain more than 15 branches. To our

Table 1. Summary of Six Possible Propagation Reactions Between End Groups and Vinyl Groups Using Apparent Propagation Rate Constants During Copolymerization of IM and IB

	Reactions
1	$C_I + V_I \xrightarrow{k_{p\mathrm{IIapp}}} C_S$
2	$C_I + V_M \xrightarrow{k_{p\mathrm{IMapp}}} C_M$
3	$C_M + V_I \xrightarrow{k_{p\mathrm{MIapp}}} C_S$
4	$C_M + V_M \xrightarrow{k_{p\mathrm{MMapp}}} C_M$
5	$C_S + V_I \xrightarrow{k_{p\mathrm{SIapp}}} C_S$
6	$C_S + V_M \xrightarrow{k_{p\mathrm{SMapp}}} C_M$

Table 2. Six Apparent Propagation Rate Constants and Their Estimated Values[2,14,15]

Parameter	Estimate	Units
$k_{p\mathrm{IIapp}}=k_{p\mathrm{II}}\times(K_0K_1[\mathrm{TiCl_4}]_0+K_0K_2[\mathrm{TiCl_4}]_0^2)$	7.5×10^{-3}	L mol^{-1} s^{-1}
$k_{p\mathrm{IMapp}}=k_{p\mathrm{IM}}\times(K_0K_1[\mathrm{TiCl_4}]_0+K_0K_2[\mathrm{TiCl_4}]_0^2)$	3.99×10^{-4}	L mol^{-1} s^{-1}
$k_{p\mathrm{MIapp}}=k_{p\mathrm{MI}}\times(K_0K_1[\mathrm{TiCl_4}]_0+K_0K_2[\mathrm{TiCl_4}]_0^2)$	0.195	L mol^{-1} s^{-1}
$k_{p\mathrm{MMapp}}=k_{p\mathrm{MM}}\times(K_0K_1[\mathrm{TiCl_4}]_0+K_0K_2[\mathrm{TiCl_4}]_0^2)$	2.126	L mol^{-1} s^{-1}
$k_{p\mathrm{SIapp}}=k_{p\mathrm{SI}}\times(K_0K_1[\mathrm{TiCl_4}]_0+K_0K_2[\mathrm{TiCl_4}]_0^2)$	1.0×10^{-4}	L mol^{-1} s^{-1}
$k_{p\mathrm{SMapp}}=k_{p\mathrm{SM}}\times(K_0K_1[\mathrm{TiCl_4}]_0+K_0K_2[\mathrm{TiCl_4}]_0^2)$	1.39×10^{-2}	L mol^{-1} s^{-1}

where $K_0=\frac{k_0}{k_{-0}}=\frac{[P_n^*\mathrm{LA}]}{[P_n][\mathrm{LA}]}$; $K_1=\frac{k_1}{k_{-1}}=\frac{[P_n^+\mathrm{LA}^-]}{[P_n^*\mathrm{LA}]}$; $K_2=\frac{k_2}{k_{-2}}=\frac{[P_n^+\mathrm{LA}_2^-]}{[P_n^*\mathrm{LA}][\mathrm{LA}]}$.

knowledge, this was the first SCVCP model in the literature that has been used for estimating a variety of model parameters that correspond to different types of end groups. Parameters $k_{p\mathrm{IMapp}}$, $k_{p\mathrm{MIapp}}$, $k_{p\mathrm{MMapp}}$, and $k_{p\mathrm{SMapp}}$ were estimated, providing a good fit of the experimental data (see Table 2).[4] Note that parameters $k_{p\mathrm{IIapp}}$ and $k_{p\mathrm{SIapp}}$ could not be estimated because the simplifying assumptions in Table 3 remove these parameters from the model. In situations involving longer reaction times and higher branching levels, the influence of these neglected parameters will become more important. One of the objectives of the current modeling work is to develop an improved PREDICI model that can be used to estimate $k_{p\mathrm{IIapp}}$ and $k_{p\mathrm{SIapp}}$ and to obtain improved estimates of $k_{p\mathrm{IMapp}}$, $k_{p\mathrm{MIapp}}$, $k_{p\mathrm{MMapp}}$, and $k_{p\mathrm{SMapp}}$. This new model should give more reliable predictions of product properties for highly branched *arb*PIB.

More recently, we developed models that use two different kinds of MC algorithms to account for the influence of all six apparent propagation rate constants on the detailed branching and MWD of the arborescent polymer.[14,15] In these MC models, assumptions 1, 2, 3, and 4 in Table 3 are not required. Our first MC model uses a traditional approach, first developed by Gillespie,[37] to track reactions and reaction times for a small sample of molecules in the batch reactor, starting at time zero and proceeding to the end of the batch. This methodology is relatively easy to develop, but requires long simulation times to achieve accurate MWD results. Our second MC model uses an advanced algorithm that combines dynamic material balances on small molecules and end-groups with advanced MC calculations to construct individual molecules.[15] This advanced MC algorithm is much more complicated than the simpler Gillespie approach, but results in an algorithm that is hundreds of times faster than the traditional MC algorithm. However, even this advanced MC algorithm is too computationally demanding for practical use in a parameter estimation scheme. As a result, our simulations obtained using both MC models relied on poorly estimated values of $k_{p\mathrm{IMapp}}$, $k_{p\mathrm{MIapp}}$, $k_{p\mathrm{MMapp}}$, and $k_{p\mathrm{SMapp}}$ obtained from our PREDICI model and educated guesses for $k_{p\mathrm{IIapp}}$ and $k_{p\mathrm{SIapp}}$.

The objective of the research described in the current article is to build an advanced PREDICI model that can provide accurate predictions for $\bar{M}_n$ and B_{kin}, even when branching levels are higher than 15 branches per molecule. Using the approach from our earlier PREDICI model (even with the restrictive assumptions in Table 3) accounting for molecules with up to 20 branches would require >200 species and >4000 reactions in PREDICI, which could not be practically implemented. As a result a different strategy is used. The development of this advanced PREDICI model is described later, followed by a parameter estimation study and simulation results.

Model Development

This advanced PREDICI model focuses on internal and dangling chain segments and overall measured characteristics (i.e., $\bar{M}_n$ and IB concentration). Although detailed MWD information for the overall polymer chains will not be predicted, this advanced PREDICI model is more convenient and more accurate for parameter estimation than our previous PREDICI model that relied on assumptions 1 to 4 in Table 3.

The basic idea of the proposed model is to simulate several parallel polymerization systems at the same time. This idea was inspired by Zargar et al.[16] who developed two parallel models to aid in the understanding of a branched RAFT copolymerization. Our first simulation focuses on end groups; the second simulation concentrates on internal segments and dangling segments in the branched polymer molecules; the third simulation determines the number average chain length of the polymer; the fourth simulation tracks the

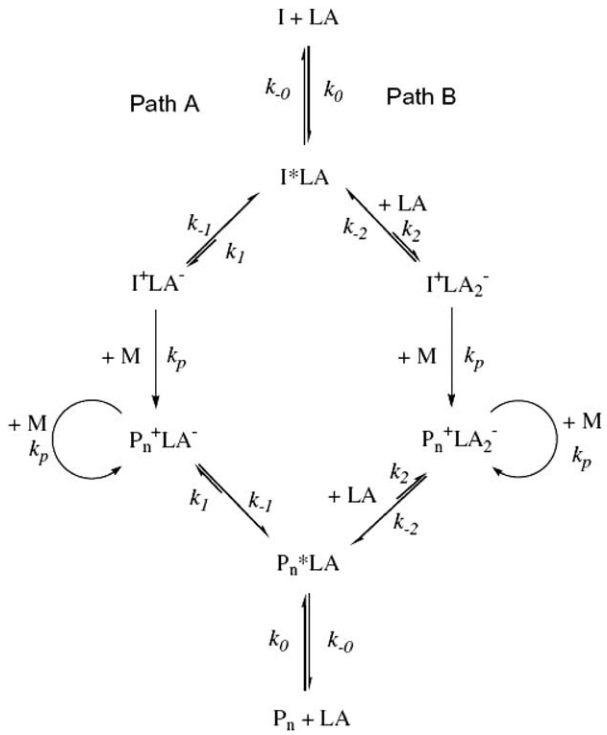

Figure 2. Two different paths for carbocationic polymerization using different amount of LA coinitiator.

Path A is dominant when LA concentration is lower than that of initiator; Path B is dominant when LA concentration is higher than that of initiator. Note I is initiator and M is monomer.[30]

Table 3. Assumptions from Our Previous PREDICI Model[2]

1	Reactions between C_I end groups and IM can be neglected because $[IM]_0$ is low relative to $[IB]_0$, so that reactions involving k_{pIIapp} can be neglected.
2	C_S end groups can only react with monomer vinyl groups. Reactions between C_S end groups and IM molecules can be neglected because IM molecules will typically initiate polymerization before their vinyl groups can be consumed by reaction. Reactions between C_S end groups and V_I groups on polymer molecules can be neglected due to steric hindrance. Because $[IM]_0$ is very low compared to $[IB]_0$, C_S groups will react with IB before they encounter the V_I groups on large molecules. Thus, reactions involving k_{pSIapp} can be neglected.
3	The C_I groups on the IM are all consumed very early in the reaction because the chloride end is designed to behave as an initiator for living carbocationic polymerization. As a result, the only reaction that IM can undergo appreciably is an initiation reaction with IB. Therefore, vinyl groups of type V_I can undergo propagation reactions only after they belong to oligomer or polymer molecules. Another consequence of this assumption is that there are no C_I groups on any polymer molecules so that reactions between polymer molecules and IM can be ignored. Note that this assumption means that there is no need to track the number of C_I groups in the model, (except for those on IM, which are consumed quickly).
4	Reactions that lead to 16 or more IM units in a molecule are neglected to keep the number of species and reactions manageable for implementation in PREDICI.
5	Puskas et al.[35] observed a penultimate effect during styrene/ IB copolymerization, indicating that the rate of IB addition to C_M may depend on whether the penultimate unit is IB or a styrene-like IM unit. Since $[IM]_0$ was low compared to $[IB]_0$ in the recipes simulated using the PREDICI model, this penultimate effect could be neglected with only a small effect on model predictions.
6	$[LA] \approx [LA]_0$ throughout the course of the batch reactions simulated using PREDICI, because only a small fraction of the $TiCl_4$ was consumed to produce ions.[36] Also, $[LA]_0$ is sufficiently large so that the MeOIM is converted instantaneously to IM at the beginning of the batch.

concentrations of small molecules and polymer chains, without paying attention to chain length. The reaction mechanisms that are considered in each of the parallel simulations are summarized in Table 4. All of the symbols are defined in the notation. Six of the rate constants shown in Table 4 are the apparent rate constants that are listed in Table 2. However, additional rate constants that are required in the third and fourth simulations are pseudo rate constants, denoted by an asterisk. For example, k^*_{pIMapp} in the second reaction in simulation 3 is the average rate constant for reaction of an IB molecule with a polymer chain of any size n_T. The overall rate of this reaction depends on the average number and type of chloride end groups on polymer molecules. As shown in Table 5, k^*_{pIMapp} can be calculated at any time using Eq. 5.1. This expression arises from the fact that the consumption rate of V_M in simulation 1 should be the same of the consumption rate of IB in simulation 3

$$-k_{pIMapp}\left[C_I^{(1)}\right]\left[V_M^{(1)}\right] = -k_{pIMapp}\left[IM^{(3)}\right]\left[IB^{(3)}\right] - k^*_{pIMapp}\left[P^{(3)}(n_T)\right]\left[IB^{(3)}\right] \quad (3)$$

Since $\left[V_M^{(1)}\right] = \left[IB^{(3)}\right]$, Eq. 3 can be rearranged to give Eq. 5.1.

Table 4. Four Parallel Polymerization Simulations That Focus on Different Arborescent Polymerization Characteristics

	Simulation 1 Chain Ends	Simulation 2 Internal and Dangling Segments	Simulation 3 Chain Length	Simulation 4 Molecules
1	$C_I^{(1)} + V_M^{(1)} \xrightarrow{k_{pIMapp}} C_M^{(1)}$	$C_I^{(2)} + V_M^{(2)} \xrightarrow{k_{pIMapp}} S_D^{(2)}(1)$	$IM^{(3)} + IB^{(3)} \xrightarrow{k_{pIMapp}} P^{(3)}(2)$	$IM^{(4)} + IB^{(4)} \xrightarrow{k_{pIMapp}} P^{(4)}$
			$P^{(3)}(n_T) + IB^{(3)} \xrightarrow{k^*_{pIMapp}} P^{(3)}(n_T+1)$	$P^{(4)} + IB^{(4)} \xrightarrow{k^*_{pIMapp}} P^{(4)}$
2	$C_M^{(1)} + V_M^{(1)} \xrightarrow{k_{pMMapp}} C_M^{(1)}$	$S_D^{(2)}(n) + V_M^{(2)} \xrightarrow{k_{pMMapp}} S_D^{(2)}(n+1)$	$P^{(3)}(n_T) + IB^{(3)} \xrightarrow{k^*_{pMMapp}} P^{(3)}(n_T+1)$	$P^{(4)} + IB^{(4)} \xrightarrow{k^*_{pMM}\text{app}} P^{(4)}$
3	$C_M^{(1)} + V_I^{(1)} \xrightarrow{k_{pMIapp}} C_S^{(1)}$	$S_D^{(2)}(n) + V_I^{(2)} \xrightarrow{k_{pMIapp}} S_I^{(2)}(n) + C_S^{(2)}$	$P^{(3)}(n_T) + IM^{(3)} \xrightarrow{k^*_{pMIapp}} P^{(3)}(n_T+1)$	$P^{(4)} + IM^{(4)} \xrightarrow{k^*_{pMIapp}} P^{(4)}$
			$P^{(3)}(n_T) + P^{(3)}(m_T) \xrightarrow{k^*_{pMIapp}} P^{(3)}(n_T+m_T)$	$P^{(4)} + P^{(4)} \xrightarrow{k^*_{pMIapp}} P^{(4)}$
4	$C_S^{(1)} + V_M^{(1)} \xrightarrow{k_{pSMapp}} C_M^{(1)}$	$C_S^{(2)} + V_M^{(2)} \xrightarrow{k_{pSMapp}} S_D^{(2)}(1)$	$P^{(3)}(n_T) + IB^{(3)} \xrightarrow{k^*_{pSMapp}} P^{(3)}(n_T+1)$	$P^{(4)} + IB^{(4)} \xrightarrow{k^*_{pSMapp}} P^{(4)}$
5	$C_S^{(1)} + V_I^{(1)} \xrightarrow{k_{pSIapp}} C_S^{(1)}$	$C_S^{(2)} + V_I^{(2)} \xrightarrow{k_{pSIapp}} C_S^{(2)} + S_I^{(2)}(0)$	$P^{(3)}(n_T) + IM^{(3)} \xrightarrow{k^*_{pSIapp}} P^{(3)}(n_T+1)$	$P^{(4)} + IM^{(4)} \xrightarrow{k^*_{pSIapp}} P^{(4)}$
			$P^{(3)}(n_T) + P^{(3)}(m_T) \xrightarrow{k^*_{pSIapp}} P^{(3)}(n_T+m_T)$	$P^{(4)} + P^{(4)} \xrightarrow{k^*_{pSIapp}} P^{(4)}$
6	$C_I^{(1)} + V_I^{(1)} \xrightarrow{k_{pIIapp}} C_S^{(1)}$	$C_I^{(2)} + V_I^{(2)} \xrightarrow{k_{pIIapp}} C_S^{(2)} + S_I^{(2)}(0)$	$IM^{(3)} + IM^{(3)} \xrightarrow{k_{pIIapp}} P^{(3)}(2)$	$IM^{(4)} + IM^{(4)} \xrightarrow{k_{pIIapp}} P^{(4)}$
			$IM^{(3)} + P^{(3)}(n_T) \xrightarrow{k_{pIIapp}} P^{(3)}(n_T+1)$	$IM^{(4)} + P^{(4)} \xrightarrow{k_{pIIapp}} P^{(4)}$
			(via V_I group on polymer)	(via V_I group on polymer)
			$P^{(3)}(n_T) + IM^{(3)} \xrightarrow{k^*_{pIIapp}} P^{(3)}(n_T+1)$	$P^{(4)} + IM^{(4)} \xrightarrow{k^*_{pIIapp}} P^{(4)}$
			(via V_I group on IM)	(via V_I group on IM)
			$P^{(3)}(n_T) + P^{(3)}(m_T) \xrightarrow{k^*_{pIIapp}} P^{(3)}(n_T+m_T)$	$P^{(4)} + P^{(4)} \xrightarrow{k^*_{pIIapp}} P^{(4)}$

Note that the apparent rate constants are applied in the coding. The number in the superscripted brackets after different species shows the simulation system the species belongs to.

Table 5. Pseudo Rate Constants Derived Using Reactions in Corresponding Rows in Table 4 for Simulations 1, 3, and 4

5.1	$k^*_{p\mathrm{IMapp}} = \frac{[C_I^{(1)}]-[\mathrm{IM}^{(3)}]}{\sum[P^{(3)}(n_T)]} k_{p\mathrm{IMapp}} = \frac{[C_I^{(1)}]-[\mathrm{IM}^{(4)}]}{[P^{(4)}]} k_{p\mathrm{IMapp}}$
5.2	$k^*_{p\mathrm{MMapp}} = \frac{[C_M^{(1)}]}{\sum[P^{(3)}(n_T)]} k_{p\mathrm{MMapp}} = \frac{[C_M^{(1)}]}{[P^{(4)}]} k_{p\mathrm{MMapp}}$
5.3	$k^*_{p\mathrm{MIapp}} = \frac{[C_M^{(1)}]}{\sum[P^{(3)}(n_T)]} k_{p\mathrm{MIapp}} = \frac{[C_M^{(1)}]}{[P^{(4)}]} k_{p\mathrm{MIapp}}$
5.4	$k^*_{p\mathrm{SMapp}} = \frac{[C_S^{(1)}]}{\sum[P^{(3)}(n_T)]} k_{p\mathrm{SMapp}} = \frac{[C_S^{(1)}]}{[P^{(4)}]} k_{p\mathrm{SMapp}}$
5.5	$k^*_{p\mathrm{SIapp}} = \frac{[C_S^{(1)}]}{\sum[P^{(3)}(n_T)]} k_{p\mathrm{SIapp}} = \frac{[C_S^{(1)}]}{[P^{(4)}]} k_{p\mathrm{SIapp}}$
5.6	$k^*_{p\mathrm{IIapp}} = \frac{[C_I^{(1)}]-[\mathrm{IM}^{(3)}]}{\sum[P^{(3)}(n_T)]} k_{p\mathrm{IIapp}} = \frac{[C_I^{(1)}]-[\mathrm{IM}^{(4)}]}{[P^{(4)}]} k_{p\mathrm{IIapp}}$

The key idea is that each pseudo rate constant must be updated over time so that all four parallel simulation systems will result in the same rates of consumption for IB and the same rates of consumption for IM. As a result, the following constraints need to be enforced at each time during the four simulations

$$\left[V_M^{(1)}\right] = \left[V_M^{(2)}\right] = \left[\mathrm{IB}^{(3)}\right] = \left[\mathrm{IB}^{(4)}\right] \tag{4}$$

$$\left[V_I^{(1)}\right] = \left[V_I^{(2)}\right] = \left[\mathrm{IM}^{(3)}\right] + \left[P^{(3)}(n_T)\right] = \left[\mathrm{IM}^{(4)}\right] + \left[P^{(4)}\right] \tag{5}$$

where the superscripts refer to the simulation that the species belongs to. Equation 4 indicates that the concentration of V_M groups is the same as the concentration of IB molecules. Equation 5 indicates that the concentration of V_I groups is the same as the sum of the concentrations of polymer molecules and unreacted IM, because each polymer molecule contains a single V_I group. Note that cyclization reactions are neglected in the current model and in our previous models.[2,14,15] Enforcing these constraints results in the expressions for the pseudo rate constants in Table 5.

The first row in Table 4 is concerned with reactions involving C_I end groups on IM or polymer molecules and the V_M group on a monomer. Simulation 1 keeps track of the resulting change in the type of end group (from C_I to C_M). Simulation 2 keeps track of the new dangling segment of length 1, $S_D^{(2)}(1)$, that arises from this type of reaction. The first row for Simulation 3 contains two reactions. The first tracks the creation of a new polymer molecule $P^{(3)}(2)$, which contains two units (one IM and one monomer) when a C_I end from an IM reacts with IB. The second tracks the growth of polymer molecules when a C_I end group from a polymer chain reacts with IB. In the fourth simulation, the first reaction in the first row tracks the increase in the number of polymer chains that occurs when IM reacts with IB. Note that the number of units in the polymer chains is not tracked in Simulation 4. The second reaction in Simulation 4 accounts for the IB that is consumed by reactions with C_I end groups on polymer chains. This reaction does not produce an additional polymer molecule.

The second row in Table 4 describes chain propagation by adding monomer to a C_M end group. Simulation 1 keeps track of the consumption of V_M groups by this chain-growth reaction. Simulation 2 tracks the propagation of dangling segments. Simulation 3 tracks the increase in chain length for the whole polymer molecule. Simulation 4 shows that the concentration of polymer chains does not change, but that IB is consumed.

Similarly, the third row accounts for the consumption of V_I groups on IM and polymer molecules by reaction with C_M end groups which produces C_S end groups. Simulation 2 tracks the conversion of a dangling segment to an internal chain segment $S_I^{(2)}(n)$ when this type of reaction occurs. Simulation 3 is interesting, because it accounts for the joining of two polymer molecules that can happen due to this type of reaction. Simulation 4 is similar, except that it does not track chain lengths.

The fourth row accounts for the creation of a new dangling segment (i.e., a branch) that occurs when a C_S end group reacts with IB. The fifth row is concerned with the consumption of V_I vinyl groups via C_S end groups. This type of reaction produces an internal segment of length zero. The sixth row in Table 4 describes the reaction between C_I end groups and V_I vinyl groups. This type of reaction also produces internal segments of length zero. Note that four different reactions are required in simulations 3 and 4 for this type of reaction, because it can occur between two IM molecules, between the C_I group on an IM and the V_I group on a polymer molecule, between the C_I group on a polymer molecule and the V_I group on an IM, or between two polymer molecules.

When developing simulation 3, we debated about the values that should be specified for some rate constants. For example, for the reaction involving two IM molecules in row 6, we initially believed that the rate constant should be $2k_{p\mathrm{IIapp}}$ rather than $k_{p\mathrm{IIapp}}$ because this reaction can happen in two ways; both IM molecules have a V_I group and a C_I group. When the concentrations of V_I groups predicted by simulation 3 did not match the results from simulation 1, we proved that the rate constant for this reaction should be $k_{p\mathrm{IIapp}}$ using the argument below. Consider the reactions

$$C_I + V_I \xrightarrow{k_{p\mathrm{IIapp}}} C_S \tag{6}$$

$$\mathrm{IM} + \mathrm{IM} \xrightarrow{k_{p?}} P \tag{7}$$

where $k_{p?}$ has an unknown value that is related to $k_{p\mathrm{IIapp}}$ so that these two reaction rates are consistent. Consider starting with 1 mol/L of IM (and nothing else) in the batch reactor. At time zero, reactions (6) and (7), which are really two ways of writing the same reaction, are the only reactions that can occur. Using these initial concentrations, the rate of consumption of V_I groups to form new polymer molecules by reaction (6) is

$$k_{p\mathrm{IIapp}}[C_I][V_I] = k_{p\mathrm{IIapp}} \tag{8}$$

Similarly, the rate of formation of new polymer molecules via reaction (7) is

$$k_{p?}[IM]^2 = k_{p?} \tag{9}$$

Equations 8 and 9 should have the same rate, as a result

$$k_{p?} = k_{p\mathrm{IIapp}} \tag{10}$$

and there is no need to multiply the apparent rate constants $k^*_{p\mathrm{MIapp}}$ by two in the third row. Similar arguments apply for $k^*_{p\mathrm{SIapp}}$ in the fifth row and $k^*_{p\mathrm{IIapp}}$ in the sixth row of Table 4.

When first developing the proposed model, we developed only simulations 1, 2, and 3. Using simulation 3, we were able to match predicted values of $\bar{M}_n$ from our MC

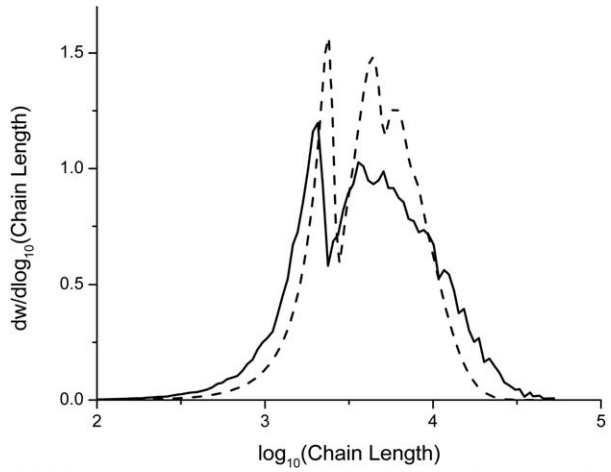

Figure 3. Comparison of the calculated MWD between simulation 3 using PREDICI and our previous advanced MC model[15] using the initial condition $[IM]_0=0.00454$ M and $[IB]_0=1.74$ M and the parameter values in Table 2. - - - is the MWD calculated by PREDICI; — is the MWD calculated by advanced MC with 10^5 polymer chains.

simulations,[14,15] but not $\bar{M}_w$ and MWD. Simulation 3 gives MWD predictions that are considerably narrower than the MWDs predicted by the MC simulations (see Figure 3). This discrepancy is caused by the implication that all polymer chains, regardless of their chain length, will have the same average reaction rate. For example, the final reaction for simulation 3 specifies that the reaction between two large chains

$$P^{(3)}(1000)+P^{(3)}(500)\xrightarrow{k^*_{p\mathrm{IIapp}}}P^{(3)}(1500) \tag{11}$$

will proceed, on average, at the same rate as a reaction between two small chains

$$P^{(3)}(10)+P^{(3)}(5)\xrightarrow{k^*_{p\mathrm{IIapp}}}P^{(3)}(15) \tag{12}$$

that react at the same time. However, for the current polymerization system, this assumption is not valid. Larger molecules tend to have more branches and, therefore, more end groups, so that reaction (11) tends to occur much more quickly than reaction (12). As a result, simulation 3 is able to accurately track the number of polymer molecules but not the chain length distribution. As a result, we decided to add simulation 4 in Table 4, which only counts the number concentration of polymer molecules in the system. The development of the number average molecular weight during the batch can be calculated from

$$\bar{M}_n=\frac{[\mathrm{IM}]_0^{(4)}-[\mathrm{IM}]^{(4)}}{[P]^{(4)}}M_{\mathrm{IM}}+\frac{[\mathrm{IB}]_0^{(4)}-[\mathrm{IB}]^{(4)}}{[P]^{(4)}}M_{\mathrm{IB}} \tag{13}$$

It is preferable to compute $\bar{M}_n$ using Eq. 13 instead of the method of moments in simulation 3, because simulation 4 requires less computational effort than simulation 3, which may be beneficial during parameter estimation. In addition, simulation 4 does not produce any misleading information about $\bar{M}_w$ and MWD, which the modeler might be tempted to believe. Results from simulation 3 are included in the current article because they serve as a warning to other researchers who might try a similar modeling approach. Note that the bimodal MWD predicted by the MC simulation in Figure 3 is consistent with bimodal distributions observed experimentally.[4,15] The low-molecular-weight peak is primarily linear polymer and the higher-molecular-weight peak results from the branched polymer molecules.

The average number of branches per polymer molecule can be determined from

$$B_{\mathrm{kin}}=\frac{[\mathrm{IM}]_0^{(4)}-[\mathrm{IM}]^{(4)}}{[P]^{(4)}}-1 \tag{14}$$

which is equivalent to Eq. 1. If there are only linear chains in the system, so that the number of IM units consumed is equal to the number of polymer molecules, the value of B_{kin} is zero. Although our initial aim was to develop a simplified PREDICI model that would predict [IB], [IM], B_{kin}, $\bar{M}_n$, $\bar{M}_w$, and MWD values, the current model (simulations 1, 2, and 4) can only predict [IB], [IM], B_{kin}, and $\bar{M}_n$. In the next section, we describe how the model predictions of [IB] and $\bar{M}_n$ can be used along with data provided by Dos Santos[4] to provide improved estimates of the model parameters.

Parameter Estimation and Simulation Results

Parameter estimation

The experimental data of Dos Santos that were used in our previous parameter estimation study are used again here to estimate all six apparent rate constants.[2,4] Recall that only four apparent rate constants ($k_{p\mathrm{IMapp}}$, $k_{p\mathrm{MMapp}}$, $k_{p\mathrm{MIapp}}$, and $k_{p\mathrm{SMapp}}$) were estimated in our previous study because $k_{p\mathrm{IIapp}}$ and $k_{p\mathrm{SIapp}}$ were eliminated due to simplifying assumptions 1 and 2 in Table 3. The initial values and uncertainty ranges for $k_{p\mathrm{IMapp}}$, $k_{p\mathrm{MMapp}}$, $k_{p\mathrm{MIapp}}$, and $k_{p\mathrm{SMapp}}$ shown in Table 6 are the same values that we used in our previous work. These values were obtained using information from the literature and our engineering judgment.[2,4,30,33,35,36,38–42] The lower and upper bounds shown were enforced during parameter estimation to ensure that estimated parameter values are physically realistic.[2] For the additional two parameters, $k_{p\mathrm{IIapp}}$ and $k_{p\mathrm{SIapp}}$, which were not considered in our previous PREDICI model, we selected the rough initial guesses of 7.5×10^{-3} and 1×10^{-4} L mol^{-1} s^{-1}shown in Table 6 that were used in our previous MC simulation studies.[14,15] These values were calculated using IM homopolymerization data.[4,43] A large range between the lower and upper bounds for these parameters is specified in Table 6 because we could not find any additional information in the literature about reasonable values for these two parameters. Note that the initial guesses are the same as the values for the lower bounds, because the IM homopolymerization data were obtained

Table 6. Initial Values and Lower and Upper Bounds Used for Estimation of Six Apparent Rate Constants

Parameter	Initial	Lower	Upper	Units
$k_{p\mathrm{IIapp}}$	7.5×10^{-3}	7.5×10^{-3}	10	L mol^{-1} s^{-1}
$k_{p\mathrm{IMapp}}$	1.58×10^{-1}	4.11×10^{-5}	4.11	L mol^{-1} s^{-1}
$k_{p\mathrm{MIapp}}$	3.16×10^{-2}	4.11×10^{-6}	4.11	L mol^{-1} s^{-1}
$k_{p\mathrm{MMapp}}$	4.58×10^{-1}	4.11×10^{-4}	4.11	L mol^{-1} s^{-1}
$k_{p\mathrm{SIapp}}$	1×10^{-4}	1×10^{-4}	10	L mol^{-1} s^{-1}
$k_{p\mathrm{SMapp}}$	2.64×10^{-4}	4.11×10^{-5}	4.11	L mol^{-1} s^{-1}

using a lower concentration of LA (i.e., $TiCl_4$) than in the copolymerization experiments that are simulated in the current article. This lower LA concentration should lead to lower values of the apparent rate constants (see Table 2) than the values that apply to the datasets used for parameter estimation.

When developing fundamental models of polymerization reactors, it is important to determine whether all of the kinetic parameters in the model should be estimated, or whether only a subset of the parameters should be estimated from the available data.[30,44–52] Estimating too many parameters using limited data leads to large uncertainty ranges for the parameters and can produce worse predictions than when fewer parameters are estimated. Conversely, estimating too few parameters can also give poor predictions, due to incorrect values that are assumed for the unestimated parameters.[53–57] In this study, advanced statistical techniques[2,52–57] are used to determine if all six parameters in Table 6 could be estimated reliably using the limited data collected by Dos Santos.[4] An orthogonalization method[52] is first used to rank all of the parameters from the most estimable to the least estimable, based on information about the influence of each parameter on predictions of the available data, uncertainties in the initial parameter values, and uncertainties in the different types of measurements. This algorithm also accounts for correlated effects of model parameters.[49,52] After the parameters are ranked, Wu's mean-squared error criterion[55] is used to decide on the appropriate number of parameters to estimate to obtain the most reliable predictions using the available data. The final parameter estimates were obtained using the following weighted nonlinear least-squares objective function

$$J=\sum \frac{([\mathrm{IB}]_{\mathrm{exp}}-[\mathrm{IB}])^2}{s^2_{\mathrm{IB}}}+\sum \frac{(\bar{M}_{n\mathrm{exp}}-\bar{M}_n)^2}{s^2_{\bar{M}_n}} \tag{15}$$

where $[\mathrm{IB}]_{\mathrm{exp}}$ and $\bar{M}_{n\mathrm{exp}}$ are the experimental measurements of the concentration of IB and the number average molecular weight, respectively. $s^2_{\mathrm{IB}}=0.01485$ mol^2 L^{-2} and $s^2_{\bar{M}_n}=313.255$ kg^2 mol^{-2} are pooled variance estimates for the IB concentration and number average molecular weight, respectively, determined from replicates experiments.[4] Note that objective function (15) contains fewer terms than the objective function used in our earlier parameter estimation study.[2] A term penalizing deviations between experimental data and the weight average molecular weight is not included in Eq. 15 because the current model, unlike our previous PREDICI model, cannot predict $\bar{M}_w$. Also, we decided to remove a term that penalizes deviations between "measured" branching level and predictions of B_{kin}. Our reason for removing the B_{kin} term from the objective function is that Dos Santos did not measure B_{kin} independently in the experiments used for parameter estimation.[4] Instead, the B_{kin} values that he reported were calculated from Eq. 1 using measured values of $\bar{M}_n$ and [IB], assuming that [IM] = 0 after the first few minutes of the reaction. Since measured values of $\bar{M}_n$ and [IB] from Dos Santos's experiments already appear in objective function (15), it is not appropriate to include an additional term that accounts for this same information in the pseudo-measurements, especially when the assumption that [IM] = 0 may not be accurate. Note that Dos Santos did measure branching levels (via a link destruction technique) for some *arb*PIB experiments, obtaining good agreement with B_{kin} calculations.[4] These data are not used for parameter estimation because we could not find sufficient information about the details of the polymer synthesis (e.g., the time at which the *arb*PIB was sampled from the batch reactor).

Parameter estimation was performed 20 times starting from different sets of initial guesses selected between the lower and upper values specified in Table 6. The first estimation was started from the initial values specified in Table 6, which are the same initial values used in our previous modeling study.[2,14,15] Starting from these values, the estimability ranking method of Yao et al.[52] and Thompson et al.[49] was used to rank the six parameters from most estimable to least estimable. Parameters $k_{p\mathrm{MMapp}}$, $k_{p\mathrm{MIapp}}$, and $k_{p\mathrm{IMapp}}$ are the top three most estimable parameters because there is a large fraction of IB units in the system (compared with IM), giving these parameters a large influence on the model predictions. Parameters $k_{p\mathrm{SMapp}}$, $k_{p\mathrm{IIapp}}$, and $k_{p\mathrm{SIapp}}$ are the least estimable because they have less influence. Wu's critical ratio was then used to determine that the top three parameters on the ranked list should be estimated and that the remaining three parameters should be held at its initial value. Estimating the top three parameters gave $J = 68.1$, which is considerably better than $J = 1349.3$ obtained using the initial parameter guesses and only slightly better than $J = 69.0$, which is obtained when the objective function is computed using parameter values employed in our previous MC simulations (see Table 2).[14,15] Using the values in Table 2 as initial guesses in the second estimation attempt resulted in a different parameter ranking, with parameter $k_{p\mathrm{MMapp}}$ appearing at the bottom of the list. This different ranking may have occurred because the value of $k_{p\mathrm{MMapp}}=2.126$ Lmol^{-1}s^{-1} was already well-estimated during our previous parameter estimation study.[2] In this case, Wu's critical ratio determined that five parameters should be estimated, resulting in $J = 29.2$ at the converged parameter values, which is much better than the value obtained starting from the previous initial parameter values.

These results illustrate that initial parameter guesses can have a large influence on parameter ranking results and parameter estimates, as noted in previous parameter estimation studies for polymerization models.[53,58] The reasons that different results can be obtained when different initial guesses are used are that polymerization models are often nonlinear with respect to the model parameters and convergence to different local minima can occur. To test whether the parameter estimates corresponding to $J = 29.2$ are reliable, a further 18 attempts at parameter ranking, selection, and estimation were performed by starting at random initial guesses between the lower and upper bounds specified in Table 6. From 8 of these 18 attempts, we found that all six parameters could be estimated from the available data, using Wu's critical ratio. In these eight attempts, one gave the best value of the objective function of $J = 28.9$. Three of the 18 attempts resulted in selection of five parameters for estimation, two of the 18 attempts selected four parameters for estimation, four attempts selected three parameters for estimation, and one attempt selected only two parameters for estimation. Additional details are provided elsewhere.[59] During some of the estimation attempts, especially when a larger number of parameters was being estimated, PREDICI gave warnings about correlation among the parameters and "too many reductions," indicating that the dataset might not contain sufficient information to estimate all of the parameters. Note that the best six attempts at parameter estimation provided values of J between 28.9 and 29.3. These six

Table 7. Parameter Ranking and Estimation Results for All Six Apparent Rate Constants

Parameter		Initial	Final value	95% Confidence Interval	Unit
1	$\boldsymbol{k_{p\mathrm{IMapp}}}$	8.00×10^{-3}	4.46×10^{-4}	$\pm 1.45 \times 10^{-4}$	L mol^{-1} s^{-1}
2	$\boldsymbol{k_{p\mathrm{MMapp}}}$	1.47×10^{0}	2.27×10^{0}	$\pm 4.88 \times 10^{-1}$	L mol^{-1} s^{-1}
3	$\boldsymbol{k_{p\mathrm{MIapp}}}$	1.14×10^{-4}	5.19×10^{-1}	$\pm 1.75 \times 10^{-1}$	L mol^{-1} s^{-1}
4	$k_{p\mathrm{IIapp}}$	2.97×10^{-2}	3.32×10^{-2}	$\pm 1.55 \times 10^{-1}$	L mol^{-1} s^{-1}
5	$k_{p\mathrm{SIapp}}$	6.26×10^{-1}	6.45×10^{-3}	$\pm 6.43 \times 10^{-2}$	L mol^{-1} s^{-1}
6	$k_{p\mathrm{SMapp}}$	2.08×10^{-1}	4.11×10^{-5}	$\pm 3.04 \times 10^{-4}$	L mol^{-1} s^{-1}

estimation attempts provided similar estimates for $k_{p\mathrm{IMapp}}$, $k_{p\mathrm{MIapp}}$, $k_{p\mathrm{MMapp}}$, and $k_{p\mathrm{SMapp}}$. However, the estimated values of $k_{p\mathrm{IIapp}}$ and $k_{p\mathrm{SIapp}}$ have more variability among these six estimations, suggesting that the data contain only limited information about these two parameters. Our difficulties in estimating these two parameters may be caused by the very

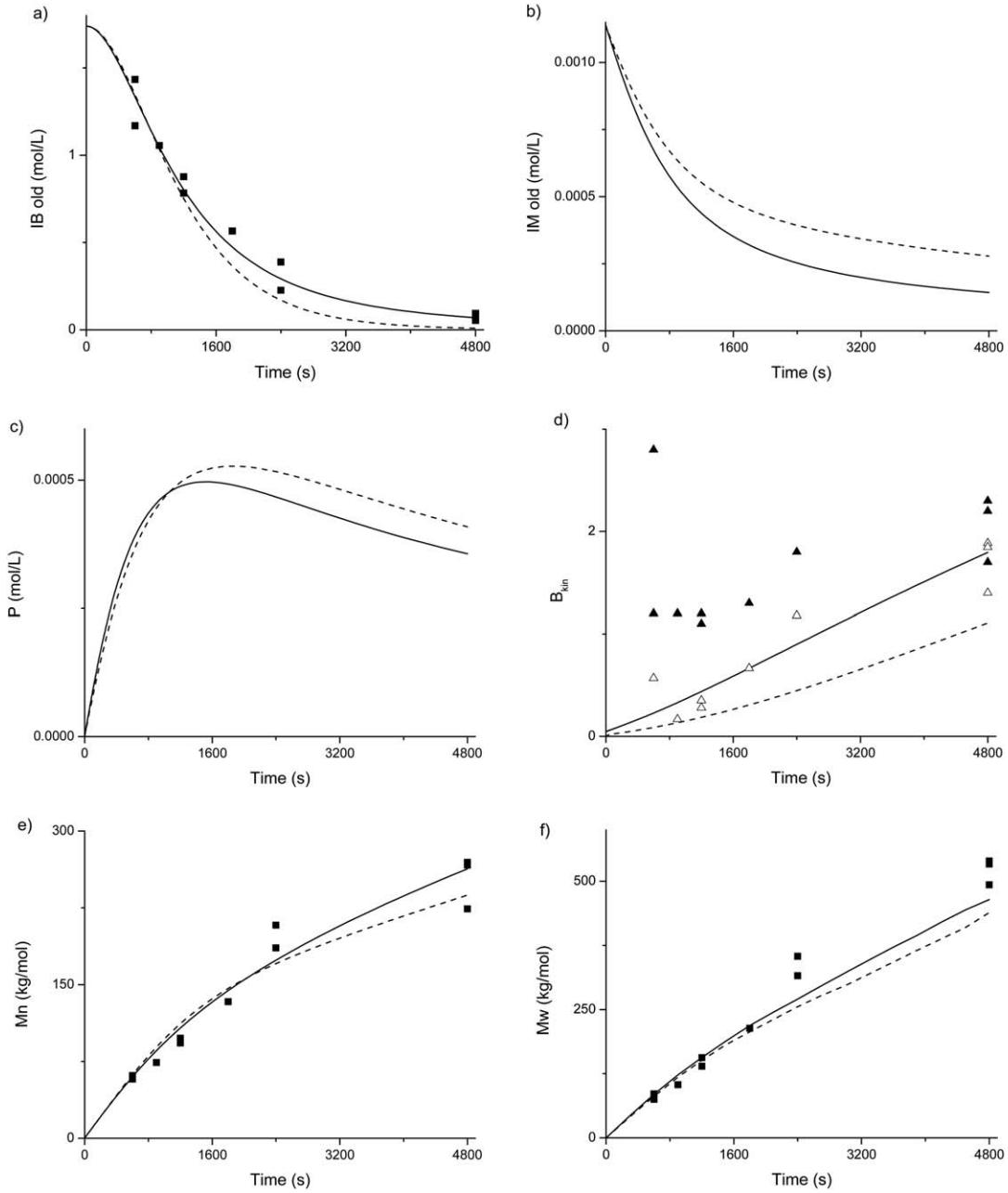

Figure 4. Comparison among experimental results and simulation results using old parameter values in Table 2 and new estimates in Table 7 for a batch reactor run with $[\mathrm{IM}]_0$=0.00114 M and $[\mathrm{IB}]_0$=1.74 M. — simulation with newly estimated parameters; - - - simulation with old parameters; ■ experimental values; ▲ B_{kin} calculated from data with assumption [IM]=0; Δ B_{kin} calculated from data using simulated [IM]; (a) [IB], (b) [IM], (c) polymer concentration, (d) B_{kin}, (e) $\bar{M}_n$, (f) $\bar{M}_w$.

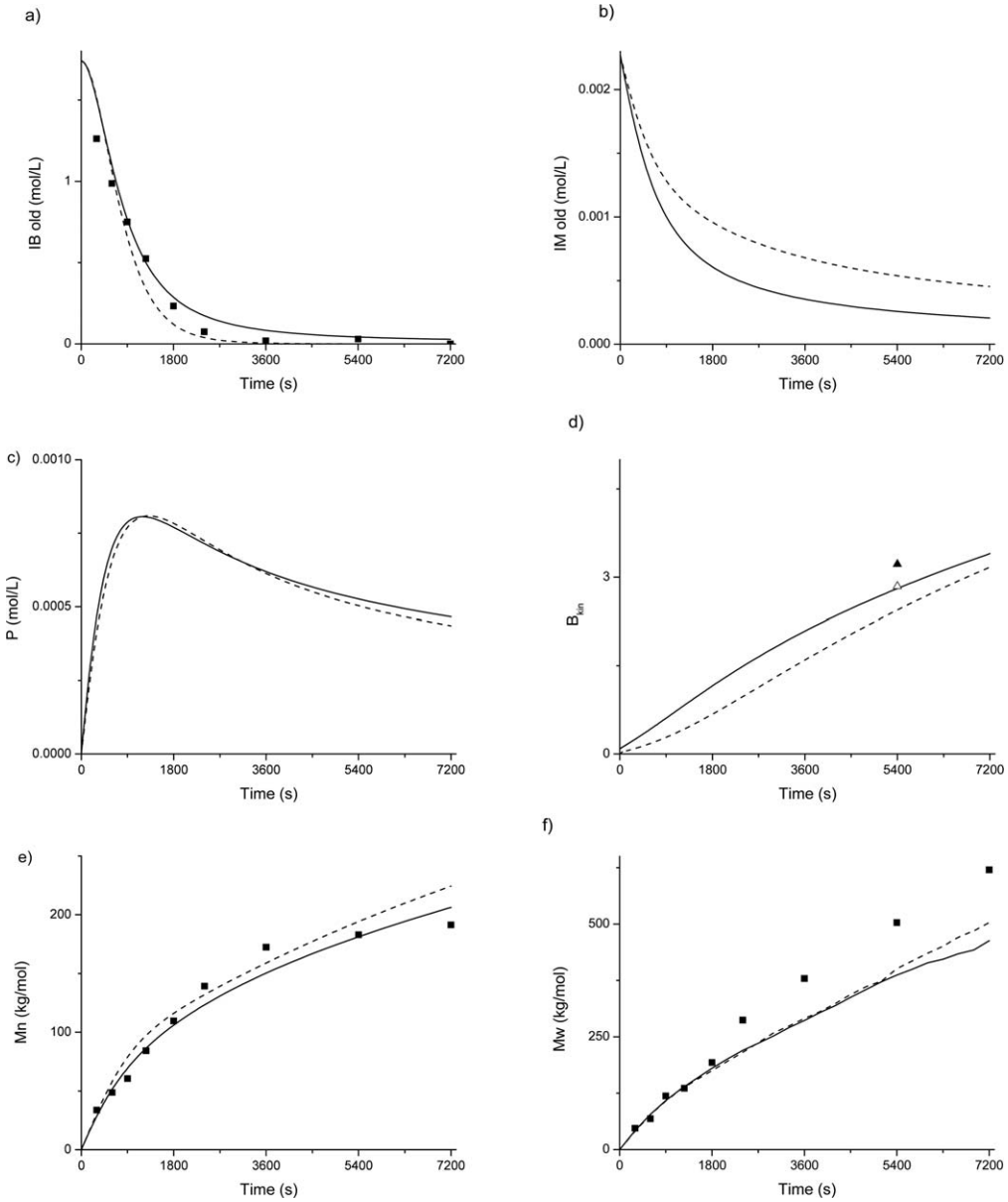

Figure 5. Comparison among experimental results and simulation results using old parameter values in Table 2 and new estimates in Table 7 for a batch reactor run with $[IM]_0=0.00227$ M and $[IB]_0=1.74$ M. — simulation with newly estimated parameters; - - - simulation with old parameters; ■ experimental values; ▲ B_{kin} calculated from data with assumption [IM]=0; Δ B_{kin} calculated from data using simulated [IM]; (a) [IB], (b) [IM], (c) polymer concentration, (d) B_{kin}, (e) $\bar{M}_n$, (f) $\bar{M}_w$.

low initial concentration of IM relative to IB (i.e., $6.55\times10^{-4} \leq \frac{[IM]_0}{[IB]_0} \leq 2.61\times10^{-3}$ in the five experimental runs used for parameter estimation). The low concentrations of IM in the system and the lack of monitoring of [IM] during the experiments provide little information for accurate fitting of $k_{p\text{IIapp}}$ and $k_{p\text{SIapp}}$. To better estimate these two parameters, it would be beneficial to obtain more experimental data from runs with higher [IM], which would lead to higher branching levels.

The best parameter values that were obtained, which correspond to $J = 28.9$ are provided in Table 7, along with approximate 95% confidence intervals. The estimates for the top three parameters in Table 7 (shown in bold) are significantly different from zero, but the other parameter estimates are not. Also, the nonoverlapping confidence intervals for $k_{p\text{IIMapp}}$, $k_{p\text{MMapp}}$, and $k_{p\text{MIapp}}$ indicate that the values of these three propagation parameters are significantly different from each other, indicating that assumptions about equal reactivities of different types of end groups and vinyl groups made by other modelers are not valid for this IB and IM copolymerization system.

These ranking and estimation results reveal that the parameters, $k_{p\text{IIapp}}$ and $k_{p\text{SIapp}}$, which were neglected in our earlier model[2] do influence the model predictions. However, these two parameters are difficult to estimate accurately. Note that the estimated values of $k_{p\text{SMapp}}$ shown in Table 7 is at the lower bound specified in Table 6. Decreasing the lower bound for $k_{p\text{SMapp}}$ during parameter estimation does not result in a noticeable improvement in the value of J.

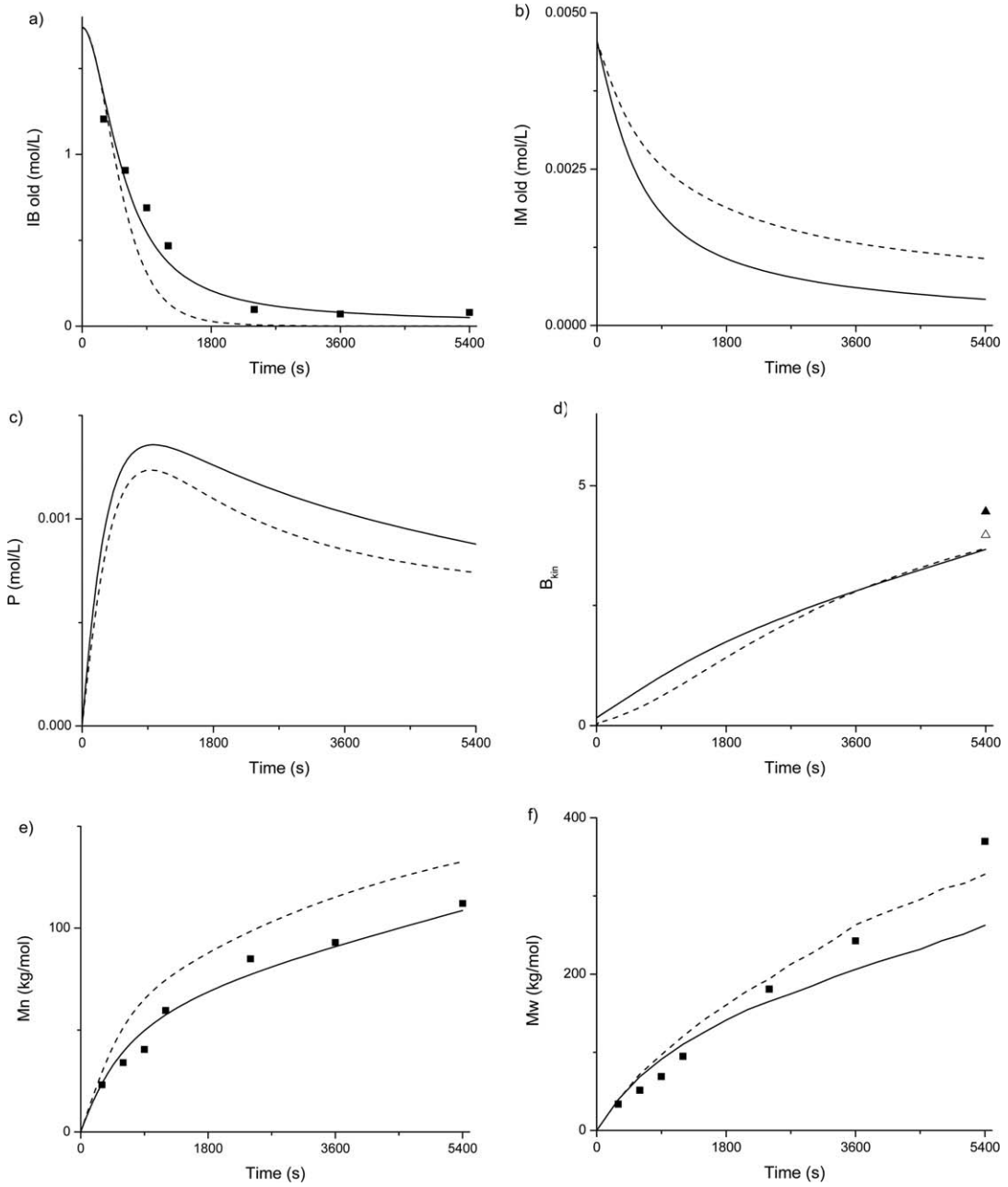

Figure 6. Comparison among experimental results and simulation results using old parameter values in Table 2 and new estimates in Table 7 for a batch reactor run with $[IM]_0=0.00454$ M and $[IB]_0=1.74$ M. — simulation with newly estimated parameters; - - - simulation with old parameters; ■ experimental values; ▲ B_{kin} calculated from data with assumption [IM]=0; Δ B_{kin} calculated from data using simulated [IM]; (a) [IB], (b) [IM], (c) polymer concentration, (d) B_{kin}, e) $\bar{M}_n$, f) $\bar{M}_w$.

Simulation results

The proposed PREDICI model requires less than 10 s to simulate a typical experimental run (see Figure 4) using a Windows 7 laptop computer with Intel Core i5 2.4 GHz and 4 GB of RAM. Figures 4–6 show comparisons between the experimental results (■ symbol) and simulation results obtained using the new estimated parameter values (solid lines) and old parameter values from Table 2 (dashed lines). Figure 4 contains replicate results obtained from three experimental runs. Note that no data are available for the IM concentrations in Figures 4b, 5b, and 6b and the polymer concentrations in Figures 4c, 5c, and 6c. In Figures 4d, 5d, and 6d, the experimental values of B_{kin} (shown using ▲) are calculated values from Eq. 1 using measurements for $\bar{M}_n$ and [IB], with [IM] assumed to be zero to match the assumption made by Dos Santos. Alternative values of B_{kin} shown using the open triangles (Δ) are computed using Eq. 1, with measured values of $\bar{M}_n$ and [IB] and the simulated value of [IM].

Figure 4 shows plots of [IB], [IM], [P], B_{kin}, $\bar{M}_n$, and $\bar{M}_w$ vs. time for a recipe with $[IM]_0=0.00114$ M and $[IB]_0=1.74$ M. Figures 5 and 6 are similar, except that they correspond to experiments with higher IM concentrations that lead to higher levels of branching. The predicted values

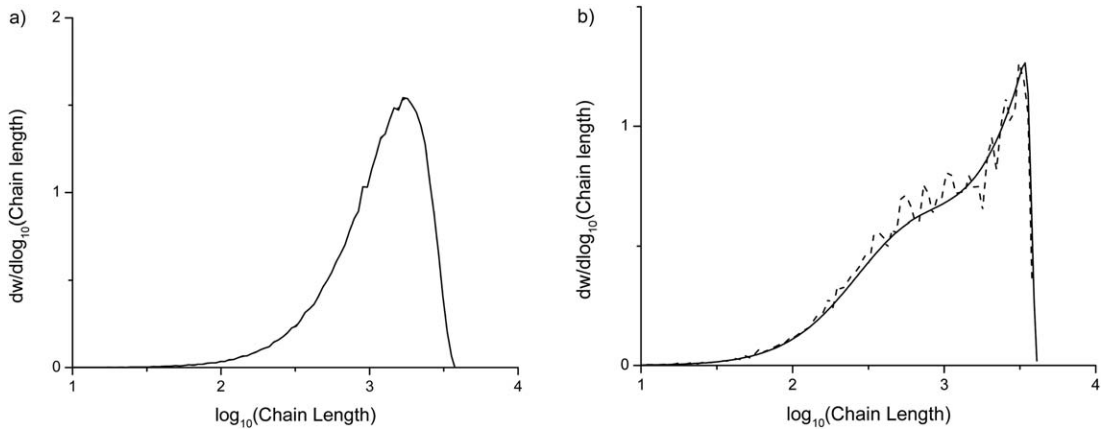

Figure 7. Predicted MWDs for (a) internal segments and (b) dangling segments at t=5400 s from experiment with $[IM]_0$=0.00454 M and $[IB]_0$=1.74 M and parameter values from Table 7; — PREDICI, -- Advanced MC. Note that the two curves in a) overlap.

of $\bar{M}_w$ were generated using the parameter estimates from the current article in our traditional MC model,[14] starting from 20,000 initial IM units and the corresponding number of IB units in the system. The MC results (not shown) agree with the other results shown in Figures 4–6. From Figures 4 to 6, it is apparent that the new estimated parameter values tend to produce better predictions of the experimental data than the old parameter values produced, particularly for [IB] and $\bar{M}_n$. In Figures 4d, 5d, and 6d, the calculated B_{kin} data (shown as Δ), using experimental values of [IB] and $\bar{M}_n$, and simulated values of [IM], are better predicted by the model than the calculated B_{kin} data from Dos Santos that assumed complete consumption of IM.[4] Predictions for $\bar{M}_w$ are also quite good using the new parameter values but are not as good as the predictions for $\bar{M}_n$ because the $\bar{M}_w$ data were not used for parameter estimation (see Eq. 15).

As shown in Figure 7, the predicted MWDs of the internal segments and dangling segments (from simulation 2) match those obtained from the advanced MC model.[15] To obtain relatively smooth MWD curves, 10^5 polymer chains were constructed using the MC calculations. The results in Figure 7a from PREDICI and the MC simulation agree very well with each other. However, in Figure 7b, results for the dangling segments agree less well because of the limited by the number of dangling segments in the MC simulation. In the 1×10^5 polymer chains that were constructed, there are 244,368 internal segments and only 9,664 dangling segments. Less jagged MC results could be obtained using a larger number of molecules. Note that it took the advanced MC model about 22 min to produce the 10^5 polymer chains and generate the MWDs in Figure 7, however, it took the proposed PREDICI model only 8.7 s to obtain the MWDs for the internal and dangling segments. Figure 7 shows that the internal segments and dangling segments tend to have similar chain lengths because most of the IB was consumed during the first 1800 s (see Figure 6a) to produce the linear segments, which could then be joined together via branching reactions later in the batch.

Conclusions

A novel model consisting of parallel simulations was developed to predict key concentrations and polymer properties in the copolymerization of IB and IM via carbocationic polymerization. The proposed dynamic model predicts changing concentrations of IB, IM, and polymer molecules, the MWDs of internal and dangling segments, and the branching level and $\bar{M}_n$ of the polymer molecules. Unlike our previous PREDICI model,[2] no restrictions on permissible branching levels needed to be introduced and all possible concentration ranges for IM and IB can be simulated. This model requires much less computational effort than previous MC models for the same copolymerization system, which makes it suitable for parameter estimation. Twenty attempts at parameter estimation were performed, starting from different initial parameter values, because some attempts converged to local minima. In each attempt, the six apparent rate constants that appear in the model were ranked from most estimable to least estimable and the number of estimable parameters was determined From eight parameter estimation attempts, it was determined that all six parameters could be estimated, for the first time, using the data of Dos Santos.[4] Nevertheless, the relatively low IM concentration and lack of [IM] monitoring in the available dataset made it difficult to obtain precise estimates of three of the six model parameters (i.e., $k_{p\text{IIapp}}$, $k_{p\text{SIapp}}$, and $k_{p\text{SMapp}}$). The newly estimated parameters result in a better fit to the data for [IB] and $\bar{M}_n$. MWD predictions for internal and dangling segments agree well with those obtained using our advanced MC model, but require significantly less computational time to determine. In the future, there is opportunity to obtain improved parameter estimates using a larger dataset that incorporates different concentrations of the LA and experiments involving IM homopolymerization.[3,43]

Acknowledgments

This contribution was identified by Dr. John R. Richards (E. I. du Pont de Nemours and Company) as the Best Presentation in the session "Modeling and Control of Polymer Processes: A Tribute to John P. Congalidis" of the 2013 AIChE Annual Meeting in San Francisco, CA. The authors thank the Natural Sciences and Engineering Research Council of Canada (NSERC) for financial support.

Notation

B_{kin} = average branching level determined from kinetic calculations and measured molecular weight
C_I = chloride-capped groups from the inimer or polymer

$C_I^{(i)}$ = chloride-capped groups from the inimer or polymer in simulation (i)
C_M = chloride-capped groups on a chain end formed after propagation with monomer
$C_M^{(i)}$ = chloride-capped groups on a chain end formed after propagation with monomer in simulation (i)
C_S = chloride-capped groups along the side of a chain, produced after propagation with an inimer vinyl group
$C_S^{(i)}$ = chloride-capped groups along the side of a chain, produced after propagation with an inimer vinyl group in simulation (i)
IB = isobutylene
$\mathrm{IB}^{(i)}$ = isobutylene in simulation (i)
$[\mathrm{IB}]_{\mathrm{exp}}$ = experimental measurements of the concentration of IB
IM = inimer, a small molecule that functions as both initiator and monomer
$\mathrm{IM}^{(i)}$ = inimer, a small molecule that functions as both initiator and monomer in simulation (i)
J = objective function value
$k_{p\mathrm{II}}$ = true rate constant for propagation reactions involving C_I and V_I
$k_{p\mathrm{IIapp}}$ = apparent rate constant for propagation reactions involving C_I and V_I
$k^*_{p\mathrm{IIapp}}$ = average rate constant defined in Table 4
$k_{p\mathrm{IM}}$ = true rate constant for propagation reactions involving C_I and V_M
$k_{p\mathrm{IMapp}}$ = apparent rate constant for propagation reactions involving C_I and V_M
$k^*_{p\mathrm{IMapp}}$ = average rate constant defined in Table 4
$k_{p\mathrm{MI}}$ = true rate constant for propagation reactions involving C_M and V_I
$k_{p\mathrm{MIapp}}$ = apparent rate constant for propagation reactions involving C_M and V_I
$k^*_{p\mathrm{MIapp}}$ = average rate constant defined in Table 4
$k_{p\mathrm{MM}}$ = true rate constant for propagation reactions involving C_M and V_M
$k_{p\mathrm{MMapp}}$ = apparent rate constant for propagation reactions involving C_M and V_M
$k^*_{p\mathrm{MMapp}}$ = average rate constant defined in Table 4
$k_{p\mathrm{SI}}$ = true rate constant for propagation reactions involving C_S and V_I
$k_{p\mathrm{SIapp}}$ = apparent rate constant for propagation reactions involving C_S and V_I
$k^*_{p\mathrm{SIapp}}$ = average rate constant defined in Table 4
$k_{p\mathrm{SM}}$ = true rate constant for propagation reactions involving C_S and V_M
$k_{p\mathrm{SMapp}}$ = apparent rate constant for propagation reactions involving C_S and V_M
$k^*_{p\mathrm{SMapp}}$ = average rate constant defined in Table 4
$k_{p?}$ = an unknown value that is related to $k_{p\mathrm{IIapp}}$
k_0 = rate constant for intermediate formation, L mol^{-1} s^{-1}
k_{-0} = rate constant for intermediate dissociation, s^{-1}
K_0 = k_0/k_{-0}, equilibrium constant for intermediate formation, L mol^{-1}
k_1 = ionization rate constant to form active species with monomeric gegenion, s^{-1}
k_{-1} = deactivation rate constant for active species with monomeric gegenion, s^{-1}
K_1 = k_1/k_{-1}, equilibrium constant for active species with monomeric gegenion
k_2 = ionization rate constant to form active species with dimeric gegenion, L mol^{-1} s^{-1}
k_{-2} = deactivation rate constant for active species with dimeric gegenion, s^{-1}
K_2 = k_2/k_{-2}, equilibrium constant for active species with dimeric gegenion, L mol^{-1}
LA = Lewis Acid
MeOIM = 4-(2-methoxyisopropyl)styrene
M_{IB} = molar mass of isobutylene
M_{IM} = molar mass of inimer
$\bar{M}_n$ = number average molecular weight
$\bar{M}_{n\mathrm{exp}}$ = experimental measurements of the number average molecular weight
$\bar{M}_{n,\mathrm{theo}}$ = theoretical number average molecular weight
$\bar{M}_w$ = weight average molecular weight
MWD = molecular weight distribution
n = number of IB units in an internal or dangling segment
n_T; m_T = total number of IB and IM units in a polymer molecule
$P^{(3)}(n_T)$ = polymer chains with n IB and IM units in total in simulation 3
$P^{(4)}$ = polymer concentrations in simulation 4
$P_n^*\mathrm{LA}$ = polymer/Lewis acid intermediate with chain of length n
$P_n^+\mathrm{LA}^-$ = active growing chain of length n, with monomeric Lewis acid gegenion
$P_n^+\mathrm{LA}_2^-$ = active growing chain of length n, with dimeric Lewis acid gegenion
SCVP = self-condensing vinyl polymerization
SCVCP = self-condensing vinyl copolymerization
$S_D^{(2)}(n)$ = dangling segment with length n in simulation 2
$S_I^{(2)}(n)$ = internal segment with length n in simulation 2
s^2_{IB} = pooled variance estimates for the isobutylene concentration
$s^2_{\bar{M}_n}$ = pooled variance estimates for the number average molecular weight
V_I = vinyl group on inimer and polymer
$V_I^{(i)}$ = vinyl group on inimer and polymer in simulation (i)
V_M = vinyl group on isobutylene
$V_M^{(i)}$ = vinyl group on isobutylene and polymer in simulation (i)

Literature Cited

1. Fréchet JMJ, Henmi M, Gitsov I, Aoshima S, Leduc MR, Grubbs RB. Self-condensing vinyl polymerization: an approach to dendritic materials. *Science*. 1995;269:1080–1083.
2. Zhao YR, McAuley KB, Puskas JE, Dos Santos LM, Alvarez A. Mathematical modeling of arborescent polyisobutylene production in batch reactors. *Macromol Theory Simul*. 2013;22:155–173.
3. Paulo C, Puskas JE. Synthesis of hyperbranched polyisobutylenes by inimer-type living polymerization. 1. Investigation of the effect of reaction conditions. *Macromolecules*. 2001;34:734–739.
4. Dos Santos LM. *Synthesis of Arborescent Model Polymer Structures by Living Carbocationic Polymerization for Structure-Property Studies [Dissertation]*. Akron, OH: University of Akron, 2009.
5. Puskas JE, Grasmüller M. Star-branched and hyperbranched polyisobutylenes. *Macromol Symp*. 1998;132:117–126.
6. Puskas JE, Kwon Y. Biomacromolecular engineering: design, synthesis and characterization. One-pot synthesis of block copolymers of arborescent polyisobutylene and polystyrene. *Polym Adv Technol*. 2006;17:615–620.
7. Puskas JE, Kwon Y, Antony P, Bhowmick AK. Synthesis and characterization of novel dendritic (arborescent, hyperbranched) polyisobutylene-polystyrene block copolymers. *J Polym Sci Part A: Polym Chem*. 2005;43:1811–1826.
8. Hong CY, Pan CY. Preparation and characterization of hyperbranched polyacrylate copolymers by self-condensing vinyl copolymerization (SCVCP). *Polym Int*. 2002;51:785–791.
9. He X, Yan D. Branched azobenzene side-chain liquid-crystalline copolymers obtained by self-condensing ATR copolymerization. *Macromol Rapid Commun*. 2004;25:949–953.
10. Liu Q, Xiong M, Cao M, Chen Y. Preparation of branched polyacrylonitrile through self-condensing vinyl copolymerization. *J Appl Polym Sci*. 2008;110:494–500.
11. Puskas JE, Dos Santos LM, Kaszas G, Kulbaba K. Novel thermoplastic elastomers based on arborescent (dendritic) polyisobutylene with short copolymer end sequences. *J Polym Sci Part A: Polym Chem*. 2009;47:1148–1158.
12. Foreman EA, Puskas JE, Kaszas G. Synthesis and characterization of arborescent (hyperbranched) polyisobutylenes from the 4-(1,2-oxirane-isopropyl)styrene inimer. *J Polym Sci Part A: Polym Chem*. 2007;45:5847–5856.
13. Heidenreich AJ, Puskas JE. Synthesis of arborescent (dendritic)polystyrenes via controlled inimer-type reversible addition-fragmentation chain transfer polymerization. *J Polym Sci Part A: Polym Chem*. 2008;46:7621–7627.
14. Zhao YR, McAuley KB, Puskas JE. Monte Carlo model for arborescent polyisobutylene production in the batch reactor. *Macromol Theory Simul*. 2013;22:365–376.
15. Zhao YR, McAuley KB, Iedema PD, Puskas JE. Advanced Monte Carlo model for arborescent polyisobutylene production in batch reactor. *Macromol Theory Simul* 2014;23:383–400.
16. Zargar A, Chang K, Taite LJ, Schork FJ. Mathematical modeling of hyperbranched water-soluble polymers with application in drug delivery. *Macromol React Eng*. 2011;5:373–384.
17. He X, Liang H, Pan C. Self-condensing vinyl polymerization in the presence of multifunctional initiator with unequal rate constants: Monte Carlo simulation. *Polymer*. 2003;44:6697–6706.

18. He X, Tang J. Kinetics of self-condensing vinyl hyperbranched polymerization in three-dimensional space. *J Polym Sci Part A: Polym Chem*. 2008;46:4486–4494.
19. He X, Liang H, Pan C. Monte Carlo simulation of hyperbranched copolymerizations in the presence of a multifunctional initiator. *Macromol Theory Simul*. 2001;10:196–203.
20. Cheng KC, Chuang TH, Chang JS, Guo W, Su WF. Effect of feed rate on structure of hyperbranched polymers formed by self-condensing vinyl polymerization in semibatch reactor. *Macromolecules*. 2005;38:8252–8257.
21. Cheng KC, Su YY, Chuang TH, Guo W, Su WF. Kinetic model of hyperbranched polymers formed by self-condensing vinyl or self-condensing ring-opening polymerization of AB monomers activated by stimuli with different reactivities. *Macromolecules*. 2010;43:8965–8970.
22. Müller AHE, Yan D, Wulkow M. Molecular parameters of hyperbranched polymers made by self-condensing vinyl polymerization. 1. Molecular weight distribution. *Macromolecules*. 1997;30:7015–7023.
23. Yan D, Müller AHE, Matyjaszewski K. Molecular parameters of hyperbranched polymers made by self-condensing vinyl polymerization. 2. Degree of branching. *Macromolecules*. 1997;30:7024–7033.
24. Litvinenko GI, Simon PFW, Müller AHE. Molecular parameters of hyperbranched copolymers obtained by self-condensing vinyl copolymerization. 1. Equal rate constants. *Macromolecules*. 1999;32:2410–2419.
25. Litvinenko GI, Simon PFW, Müller AHE. Molecular parameters of hyperbranched copolymers obtained by self-condensing vinyl copolymerization, 2. Non-equal rate constants. *Macromolecules*. 2001;34:2418–2426.
26. Litvinenko GI, Müller AHE. Molecular weight averages and degree of branching in self-condensing vinyl copolymerization in the presence of multifunctional initiators. *Macromolecules*. 2002;35:4577–4583.
27. Lim GT, Puskas JE, Reneker DH, Jakli A, Horton WE Jr. Highly hydrophobic electrospun fiber mats from polyisobutylene-based thermoplastic elastomers. *Biomacromolecules*. 2011;12:1795–1799.
28. Lim GT, Valente SA, Hart-Spicer CR, Evancho-Chapman MM, Pusaks JE, Horne WI, Schmidt SP. New biomaterial as a promising alternative to silicone breast implants. *J Mech Behav Biomed Mater*. 2013;21:47–56.
29. Puskas JE, Foreman-Orlowski EA, Lim GT, Porosky SE, Evancho-Chapman MM, Schmidt SP, Fray ME, Prowans P, Lovejoy K. A nanostructured carbon-reinforced polyisobutylene-based thermoplastic elastomer. *Biomaterials*. 2010;31:2477–2488.
30. Puskas JE, Shaikh S, Yao KZ, McAuley KB, Kaszas G. Kinetic simulation of living carbocationic polymerizations. II. Simulation of living isobutylene polymerization using a mechanistic model. *Eur Polym J*. 2005;41:1–14.
31. Kaszas G, Puskas JE. Kinetics of the carbocationic homopolymerization of isobutylene with reversible chain termination. *Polym React Eng*. 1994;2:251–273.
32. Puskas JE, Lanzendorfer MG. Investigation of the TiCl4 reaction order in living isobutylene polymerization. *Macromolecules*. 1998;31:8684–8690.
33. Puskas JE, Peng H. Kinetic simulation of living carbocationic polymerizations I. Simulation of living isobutylene polymerization. *Polym React Eng*. 1999;7:553–576.
34. Puskas JE, Dos Santos LM, Fischer F, Götz C, Fray ME, Altstädt V, Tomkins M. Fatigue testing of implantable specimens: effect of sample size and branching on the dynamic fatigue properties of polyisobutylene-based biomaterials. *Polymer*. 2009;50:591–597.
35. Puskas JE, Chain SWP, McAuley KB, Kaszas G, Shaikh S. Living carbocationic copolymerization of isobutylene with styrene. *J Polym Sci Part A: Polym Chem*. 2007;45:1778–1787.
36. Schlaad H, Kwon Y, Sipos L, Faust R, Charleux B. Determination of propagation rate constants in carbocationic polymerization of olefins. *1. Isobutylene*. *Macromolecules*. 2000;33:8225–8232.
37. Gillespie DT. Exact stochastic simulation of coupled chemical reactions. *J Phys. Chem*. 1977;81(25):2340–2361.
38. Sipos L, De P, Faust R. Effect of temperature, solvent polarity, and nature of Lewis acid on the rate constants in the carbocationic polymerization of isobutylene. *Macromolecules*. 2003;36:8282–8290.
39. De P, Faust R, Schimmel H, Ofial A, Mayr H. Determination of rate constants in the carbocationic polymerization of styrene: effect of temperature, solvent polarity, and Lewis acid. *Macromolecules*. 2004;37:4422–4433.
40. Roth M, Mayr H. A novel method for the determination of propagation rate constants: carbocationic oligomerization of isobutylene. *Macromolecules*. 1996;29:6104–6109.
41. De P, Faust R. Determination of the absolute rate constants of propagation for ion pairs and free ions in the living cationic polymerization of isobutylene. *Macromolecules*. 2005;38:9897–9900.
42. Puskas JE, Kaszas G, Kennedy JP, Kelen T, Tudos F. Quasiliving carbocationic polymerization. IX. Forced ideal copolymerization of styrene derivatives. *J Polym Sci Part A: Polym Chem*. 1982;18:1315–1338.
43. Dos Santos LM, Puskas JE. Self-condesing vinyl polymerization of 4-(2-methoxy-isopropyl)styrene. *Polym Prepr*. 2008;49:87–88.
44. Woloszyn JD, Hesse P, Hungenberg KD, McAuley KB. Parameter selection and estimation techniques ina styrene polymerization model. *Macromol React Eng*. 2013;7:293–310.
45. Woloszyn JD, McAuley KB. Application of parameter selection and estimation techniques in a thermal styrene polymerization model. *Macromol React Eng*. 2011;5:453–466.
46. Karimi H, Schaffer MA, McAuley KB. A kinetic model for non-oxidative thermal degradation of nylon 66. *Macromol React Eng*. 2012;6:93–109.
47. Cui WJ, McAuley KB, Whitney RA, Spence RE, Xie T. Mathematical model of palyether production from 1,3-propanediol. *Macromol React Eng*. 2013;7:237–253.
48. Cui WJ, McAuley KB, Spence RE, Xie T. Assesment of mass-transfer effects during polyether production from 1,3-propanediol. *Macromol React Eng*. 2014;8:476–492.
49. Thompson DE, McAuley KB, McLellan PJ. Parameter estimation in a simplified MWD model for HDPE produced by a Ziegler-Natta catalyst. *Macromol React Eng*. 2009;3:160–177.
50. Kou B, McAuley KB, Hsu CC, Bacon DW, Yao KZ. Mathematical model and parameter estimation for gas-phase ethylene homopolymerization with supported metallocene catalyst. *Ind Eng Chem Res*. 2005;44:2428–2442.
51. Kou B, McAuley KB, Hsu JCC, Bacon DW. Mathematical model and parameter estimation for gas-phase ethylene/hexane copolymerization with metallocene catalyst. *Macromol Mater Eng*. 2005;290:537–557.
52. Yao ZK, Shaw BM, Kou B, McAuley KB, Bacon DW. Modeling ethylene/butane copolymerization with multi-site catalysts: parameter estimability and experimental design. *Polym React Eng*. 2003;11:563–588.
53. McLean KAP, Wu S, McAuley KB. Mean-squared-error methods for selecting optimal parameter subsets for estimation. *Ind Eng Chem Res*. 2012;51:6105–6115.
54. McLean KAP, McAuley KB. Mathematical modeling of chemical processes-obtaining the best model predictions and parameter estimates using identifiability and estimability procedures. *Can J Chem Eng*. 2012;90:351–366.
55. Wu S, McLean KAP, Harris TJ, McAuley KB. Selection of optimal parameter set using estimability analysis and MSE-based model-selection criterion. *Int J Adv Mechatronic Syst*. 2011;3:188–197.
56. Wu S, McAuley KB, Harris TJ. Selection of simplified models: I. Analysis of model-selection criteria using mean-squared error. *Can J Chem Eng*. 2011;1:148–158.
57. Wu S, McAuley KB, Harris TJ. Selection of simplified models: II. Development of a model selection criterion based on mean squared error. *Can J Chem Eng*. 2011;89:325–336.
58. Polic AL, Lona LMF, Duever TA, Penlidis A. A protocol for the estimation of parameters in process models: case studies with polymerization scenarios. *Macromol Theory Simul*. 2004;13:115–132.
59. Zhao, YR. *Mathematical Modeling of Arborescent Polyisobutylene Production in Batch Reactor Using Novel Material Balance and Monte Carlo Methods [dissertation]*. Kingston, Ontario, Canada: Queen's University, 2014.

Manuscript received July 10, 2014, and revision received Sep. 11, 2014.